Machine and deep learning based identification of organs within LiDAR scans of tree canopies :

Application to the estimation of apple production.

Artzet Simon, Juan-Pablo Rojas-Bustos, Benoît Pallas, Evelyne Costes, Frederic Boudon

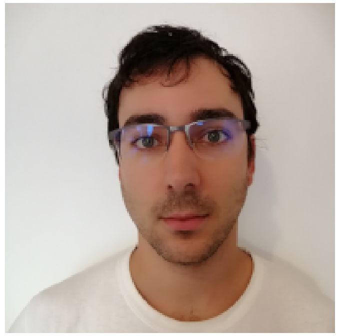    

H2020 INVITE project

INRAE cirad invite

Context - Demonstrate applicability of phenotypic tools in field test conditions for variety testing

- **INVITE** : **IN**novations in plant **V**ar**I**ety **T**esting in **E**urope
- Test a set of phenotyping tools for tree performance during variety evaluation
- Setup a novel software tools based on machine learning to automatically achieve measurement from images or LiDAR

The Riegl VZ400
LiDAR used in Montpellier

Context - Collection of diversity - Apple tree LiDAR scan

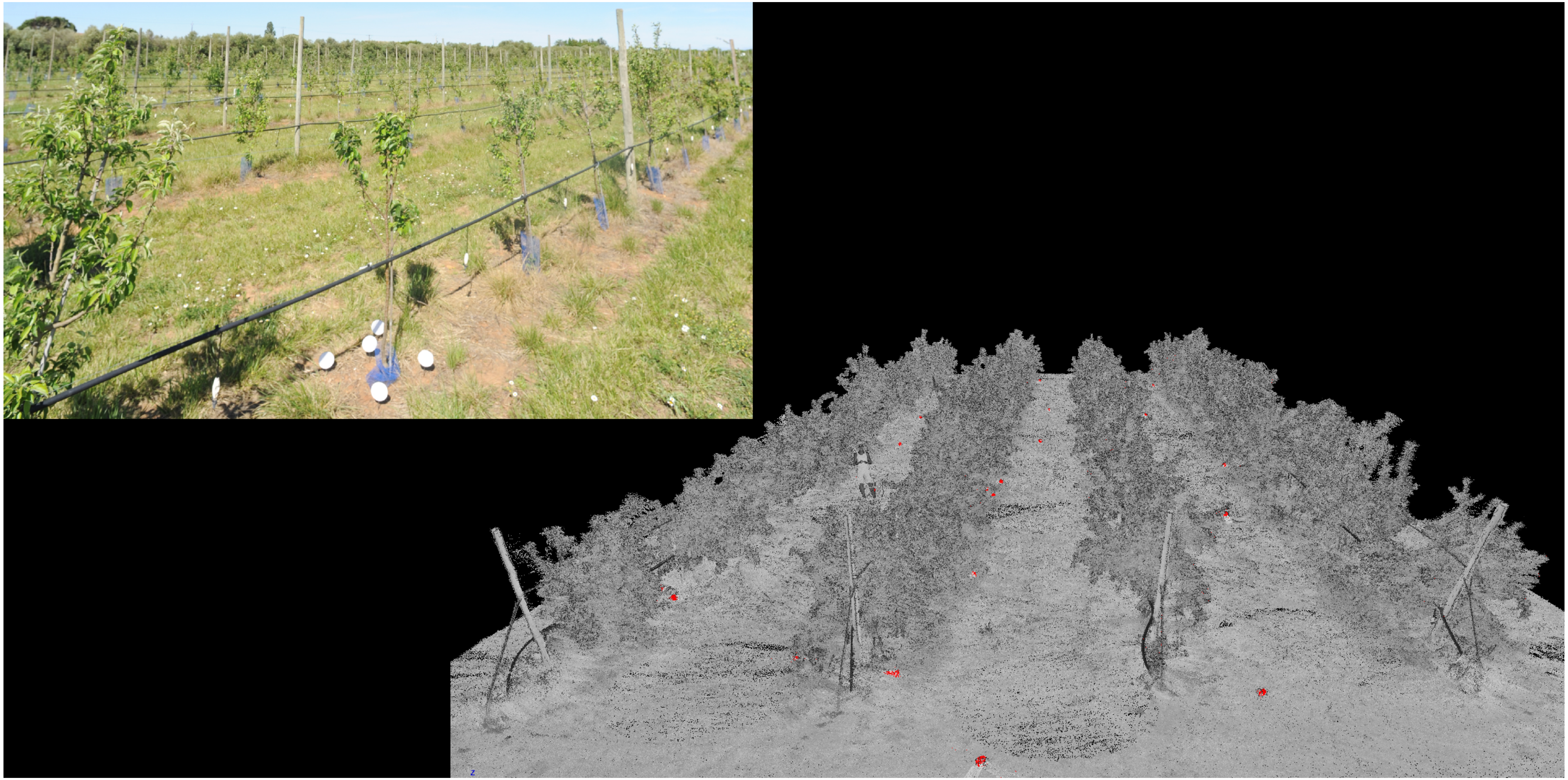

Context - Previous work on architectural characterisation

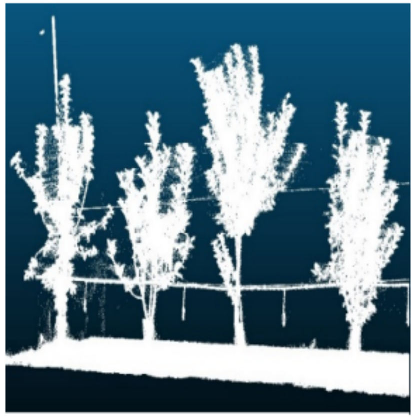

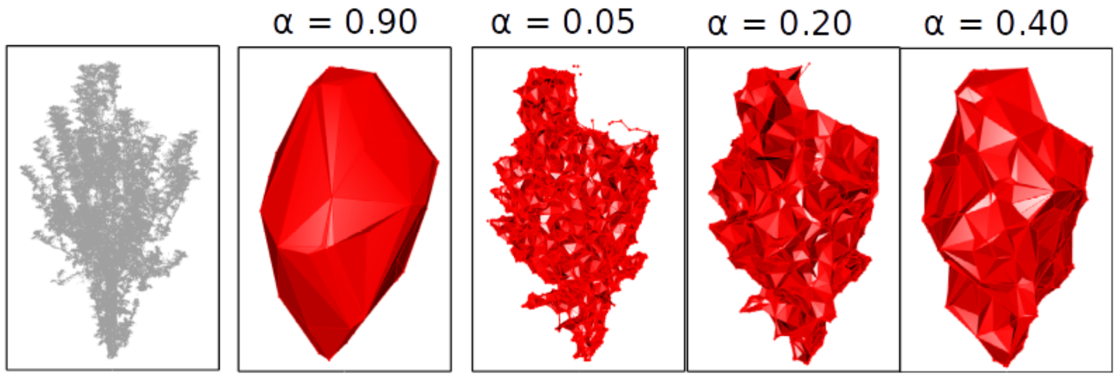

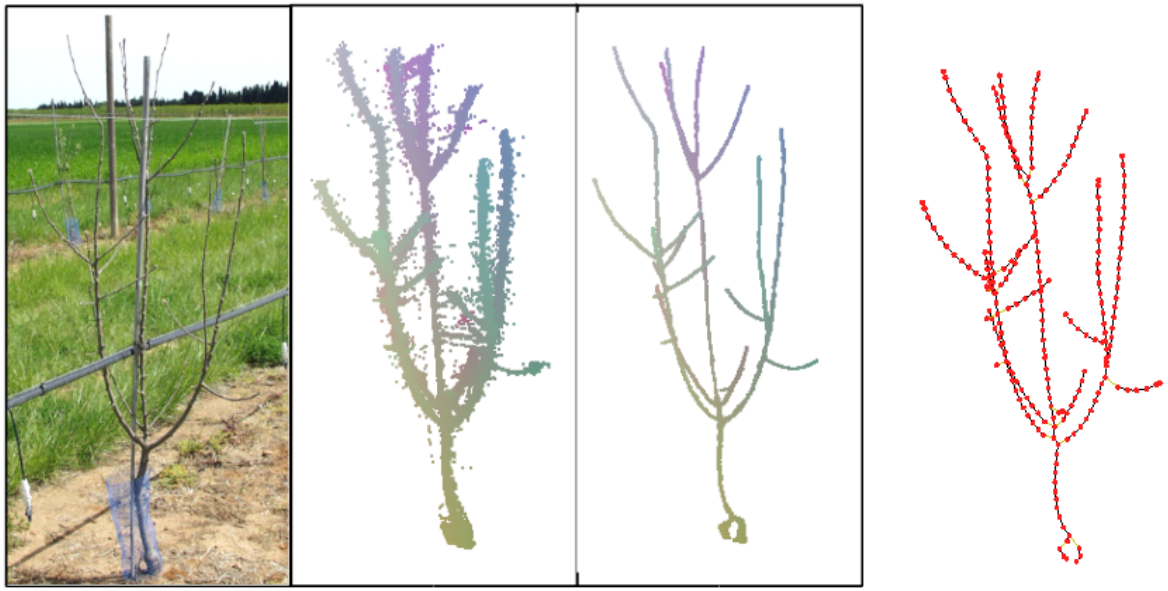

Coupel-Ledru et al. 2019

Goal - Apple Detection

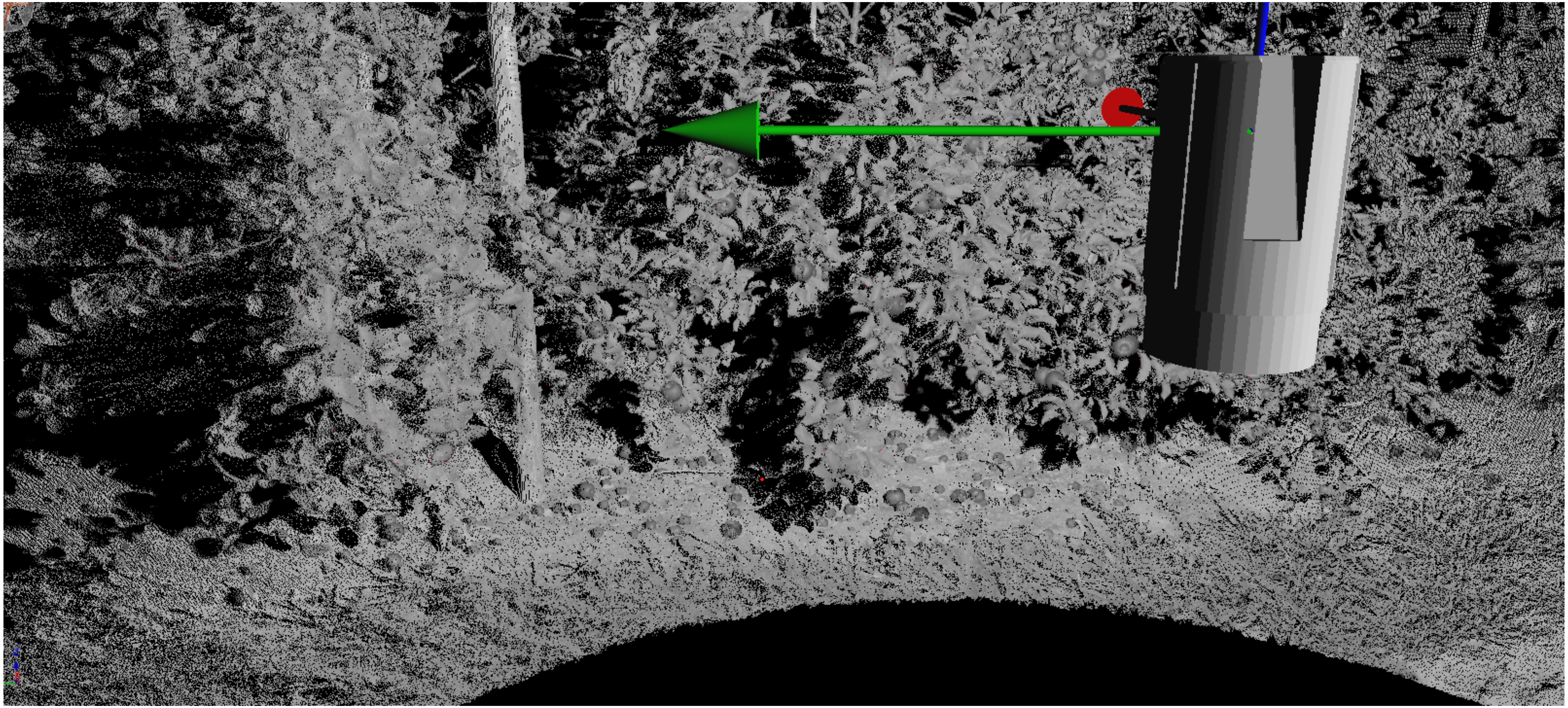

State of the art of LiDAR phenotyping and 3D recognition

LiDAR Phenotyping

- Machine learning methods start to be applied
  - **Illia Ziamtsov et Saket Navlakha**, 2019
- Only on commercial orchard
  - **Gene-Mola et al.**, 2019
  - **Tsoulias et al.**, 2020

3D recognition

- Deep learning outperform machine learning
  - **Guo, Wang, Hu, Liu et al.**, 2020
- Best prediction model are only applied to outdoor and indoor objet like car, building, table, etc.
  - **Hu et al.**, 2020

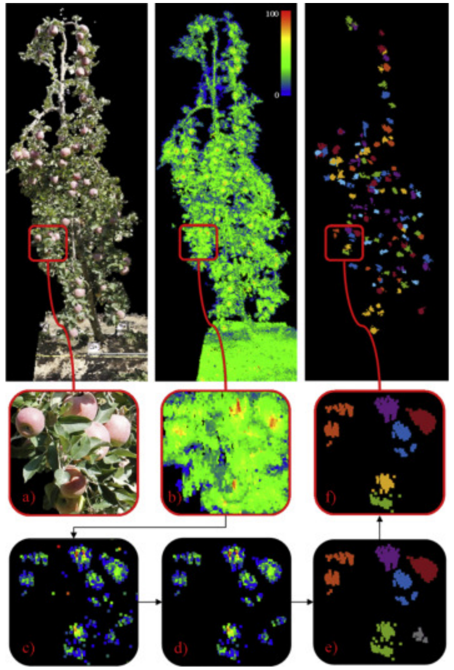

Gene-Mola et al. 2019

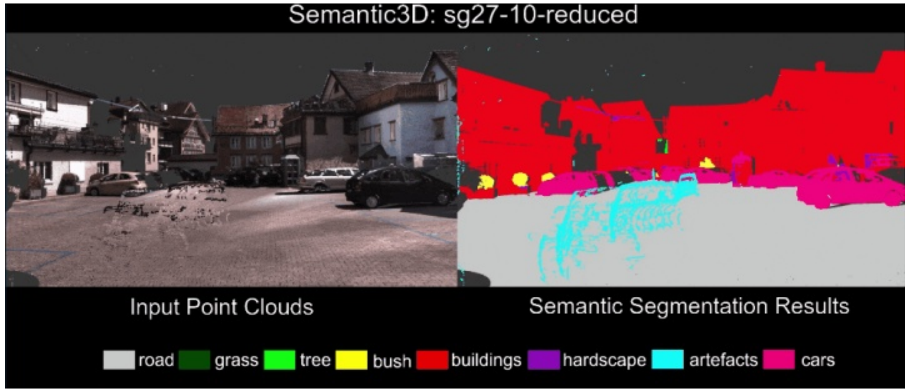

Hu et al. 2020

Comparison between machine and deep learning pipelines

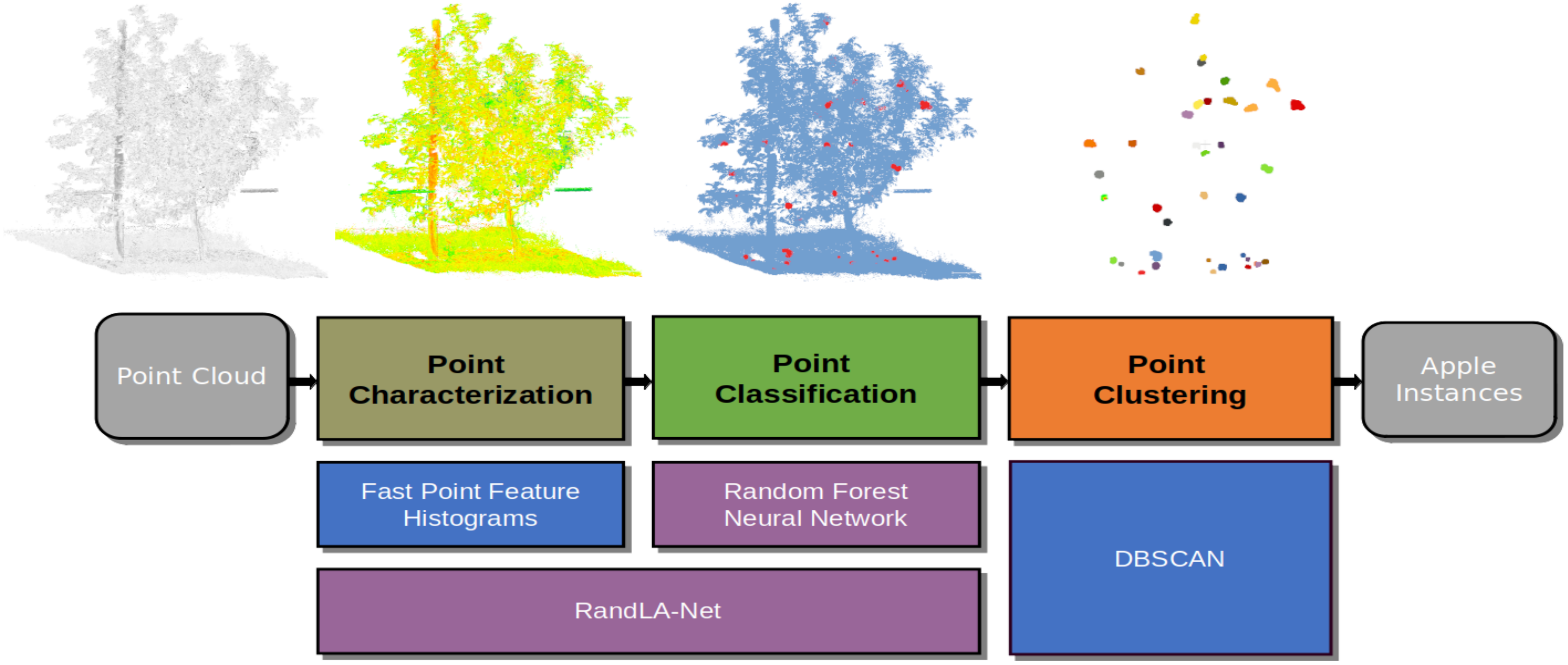

Data

Field & Synthetic

Dataset - LiDAR scans and meta-data

RAW SCAN:

- 2018 and 2019 : **320** tree scanned
  - Core collection of 250 genotypes
  - Trees not pruned

Harvest data

- Total weight of the fruits per tree
- Mean weigth of fruits (based on 50 fruits)
  - **Number of fruits**
    - Used for pipeline validation
- Genotype, date, ...

LiDar Information

- X, Y, Z
- **Reflectance**
- Deviation
- Amplitude

Two LiDAR acquisition protocols

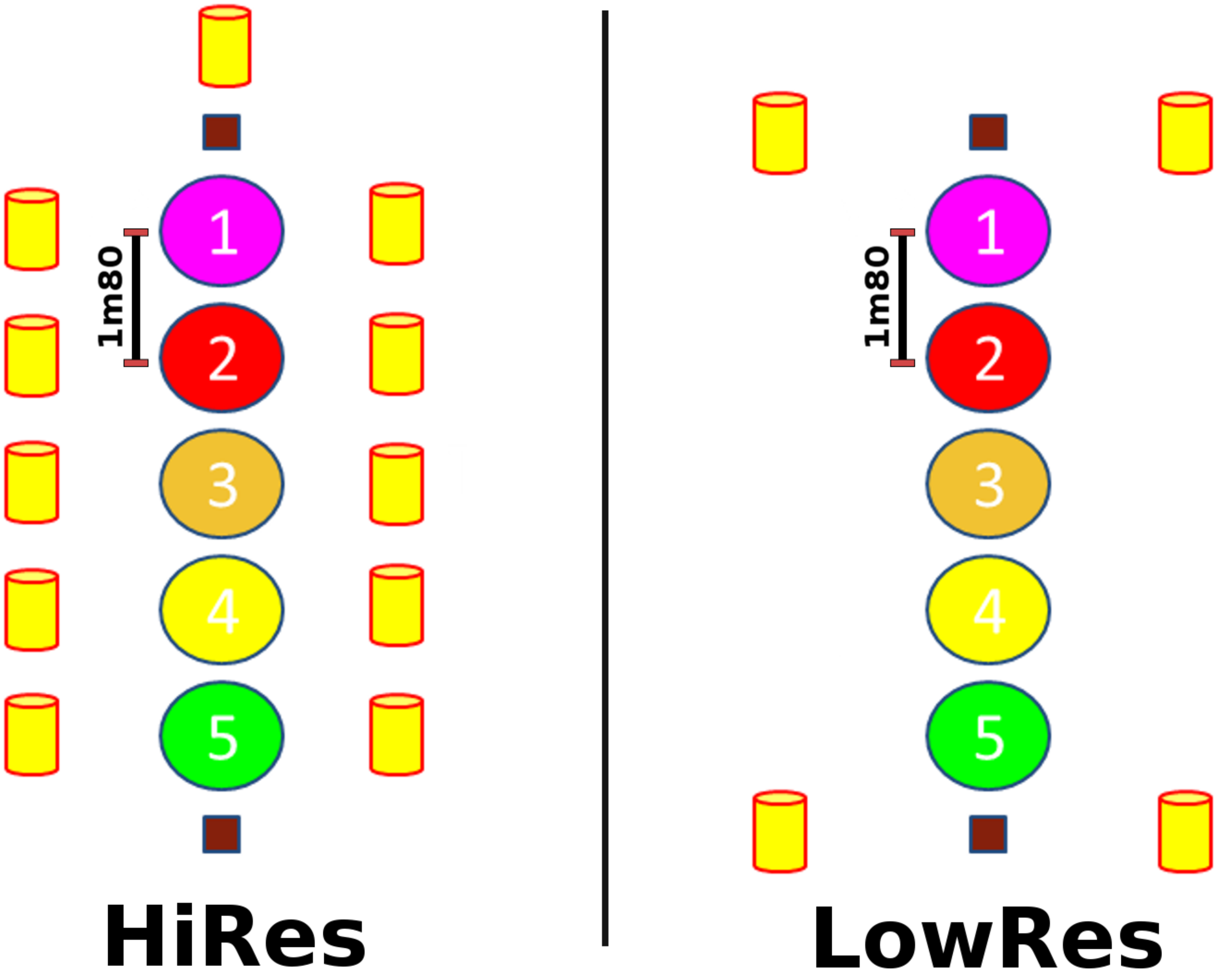

Point density - Top view

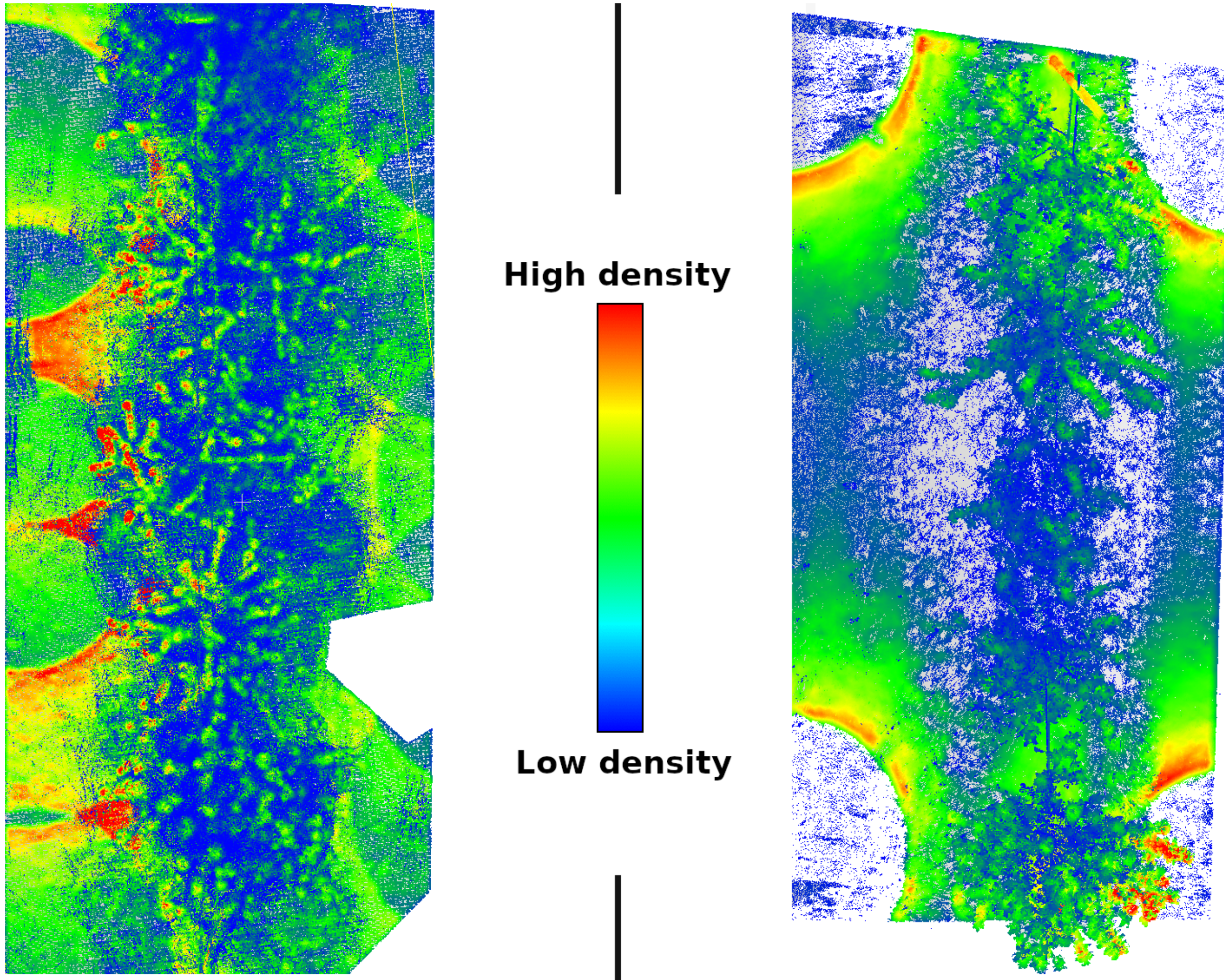

HiRes

LowRes

Point density - Top view

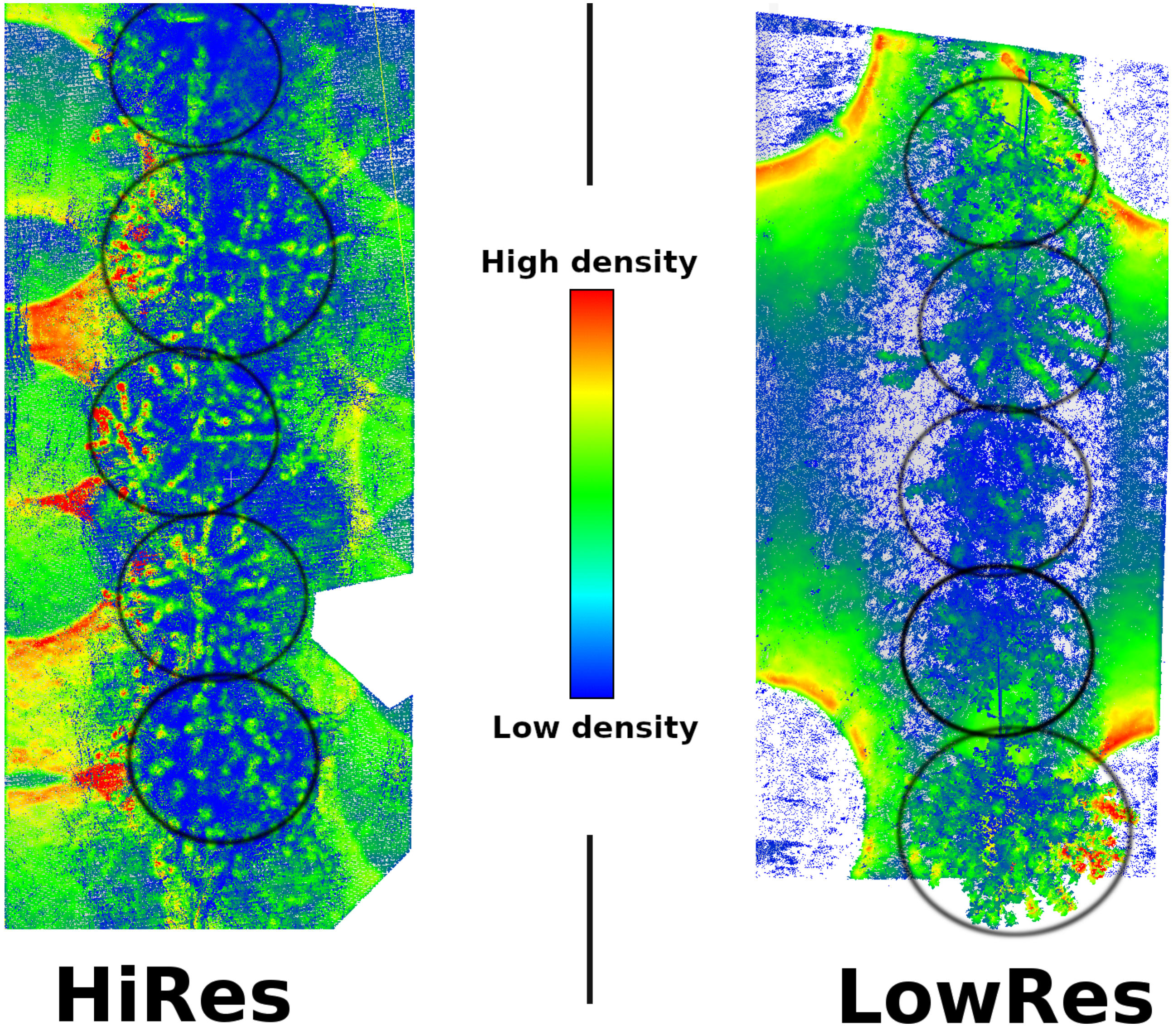

Challenge for fruit detection

- LiDAR noise
- Tree, leaf and branch occlusion :
  - Variational density
- Wind
  - Apple shape deformation
  - Branch and leaf duplication
- Trees are not pruned
  - Almost all trees are mix together

Synthetic data - MappleT + PlantGL - LiDAR Simulation

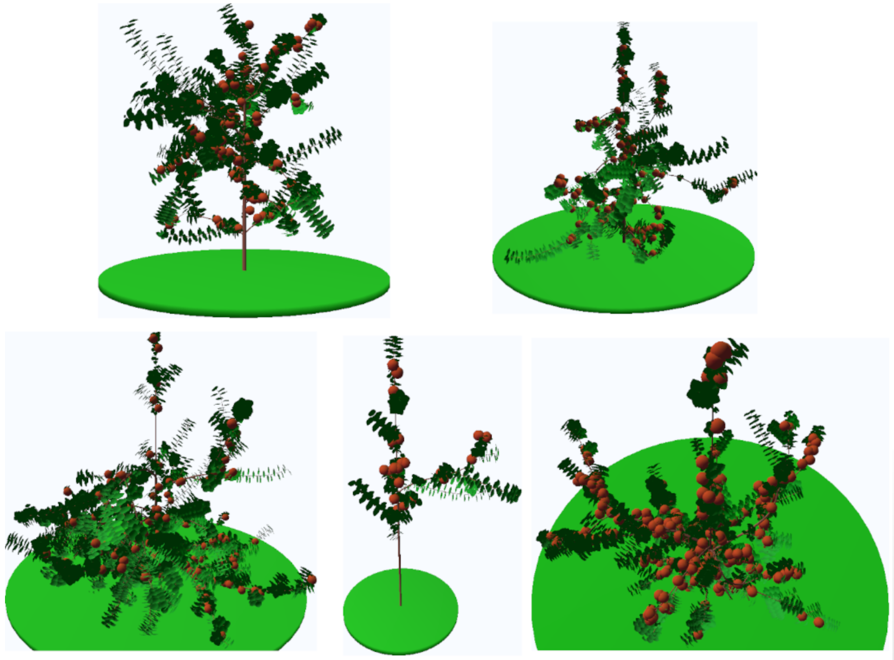

Costes et al. 2008

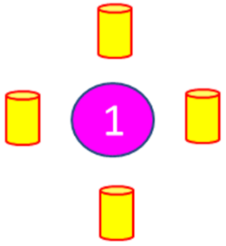

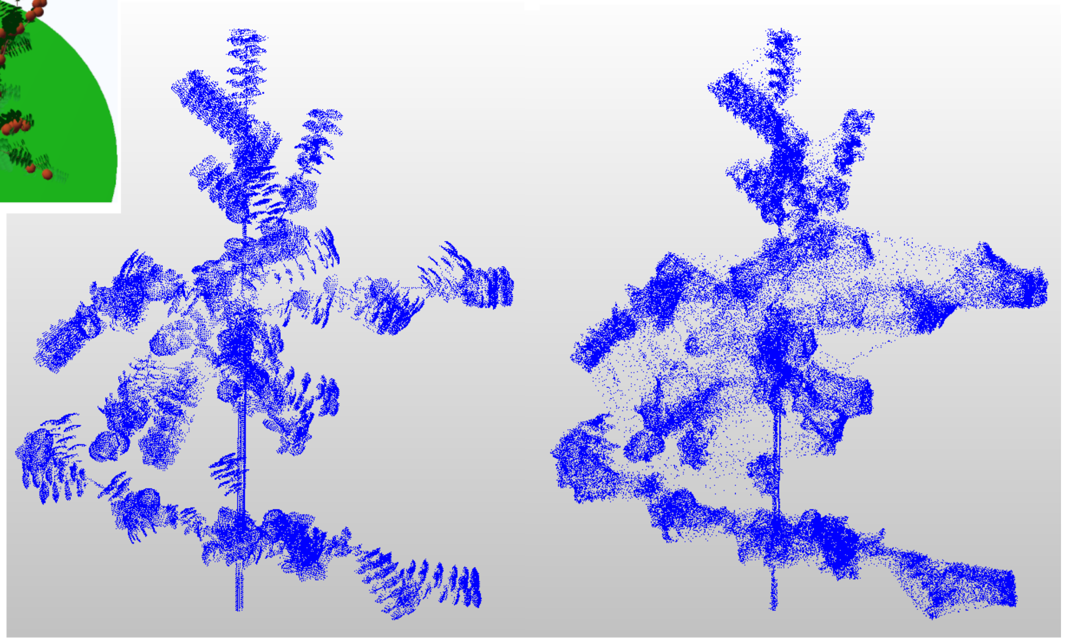

Boudon et al., 2014

DataSet - Labeled data for Training & Test

Field - 10/320 labeled trees

- **9**/290 from **4 Scans - LowRes**
  - Number of points : ~ **10M**
- **1**/31 from **11 Scans - HiRes**
  - Number of points : ~ **2.5M**

Synthetic - N (100/250) simulate trees

- **Scan every 90° - VeryHiRes**
  - Number of points : **12M**

Umbalanced data : Apple point are under-represented, a hundred times less that the other point

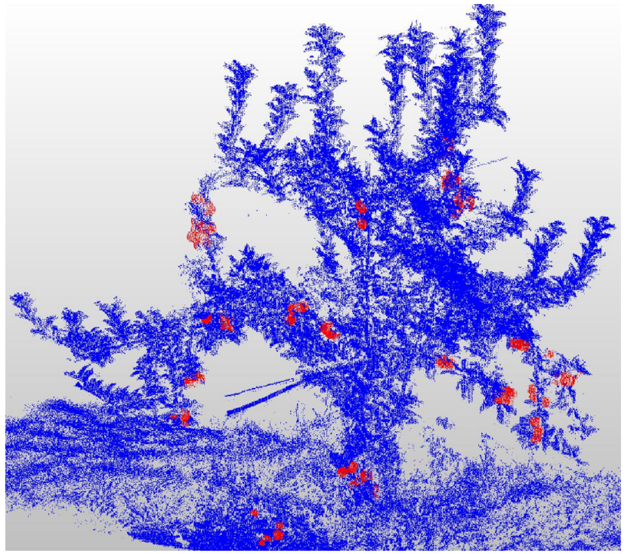

Field - LowRes

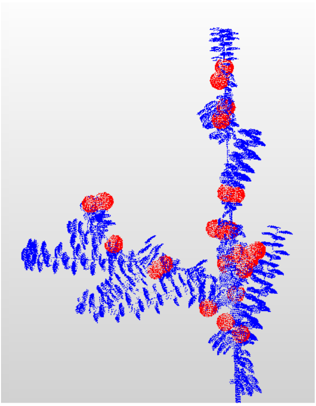

Synthetic - VeryHiRes

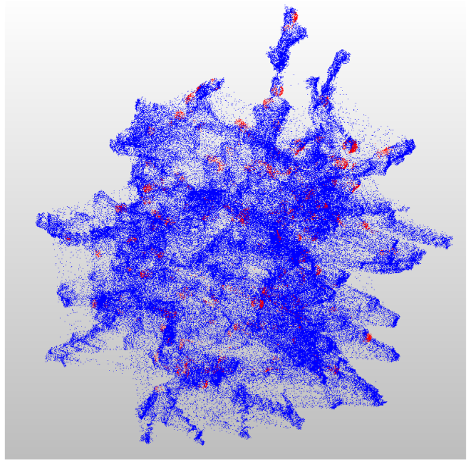

Synthetic - VeryHiRes Noised

Methods

Two pipelines based on machine and deep Learning

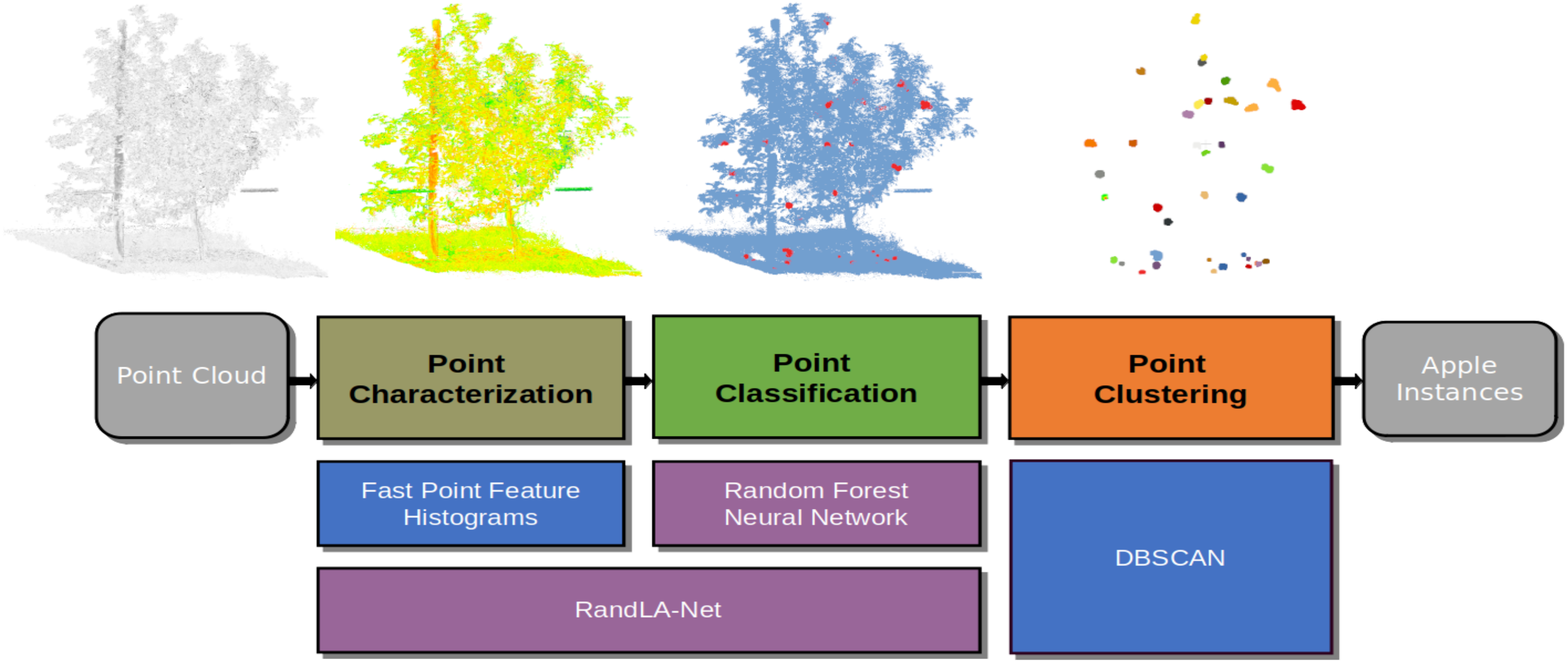

Two pipelines based on machine and deep Learning

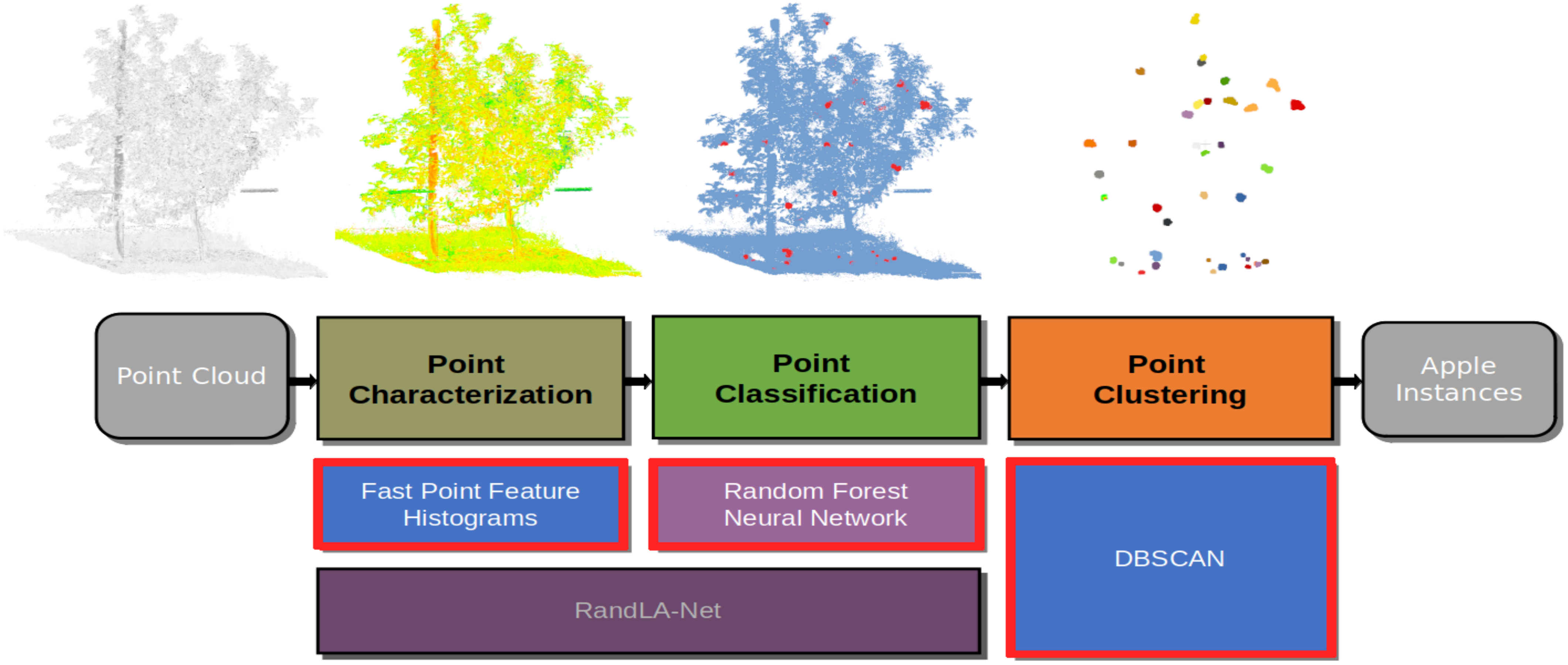

Two pipelines based on machine and deep Learning

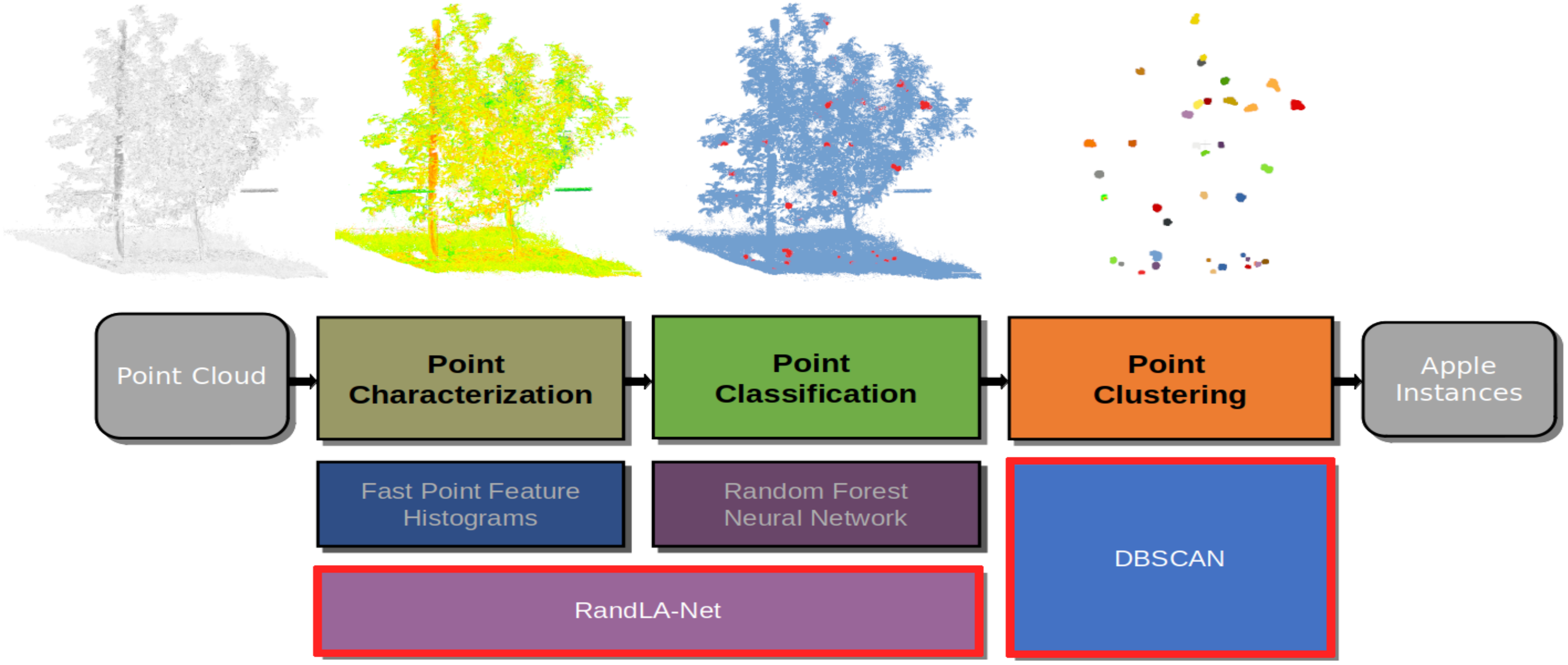

3D Geometric Features - Fast Point Features Histogram (FPFH)

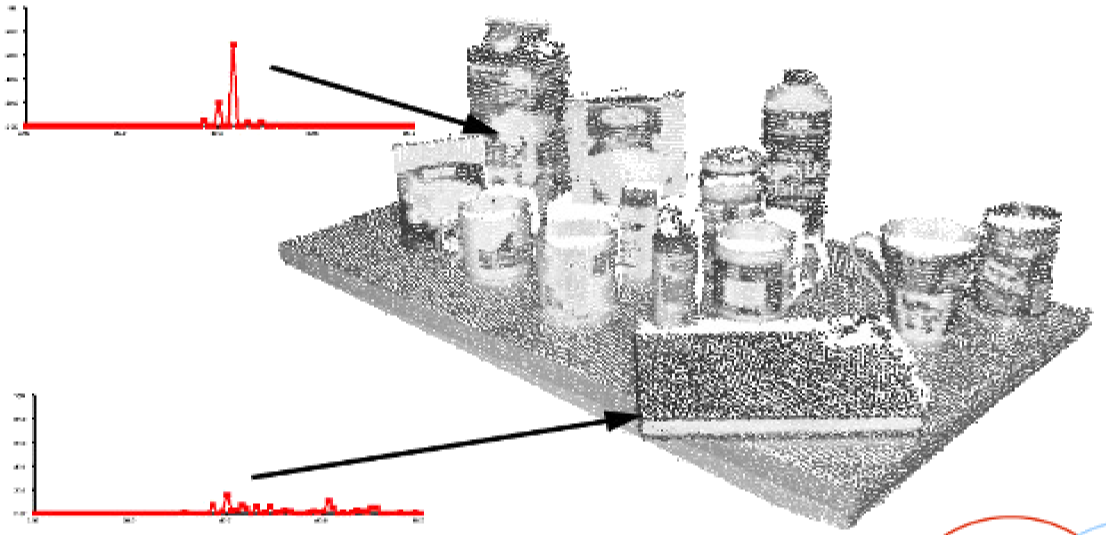

Point Characterization

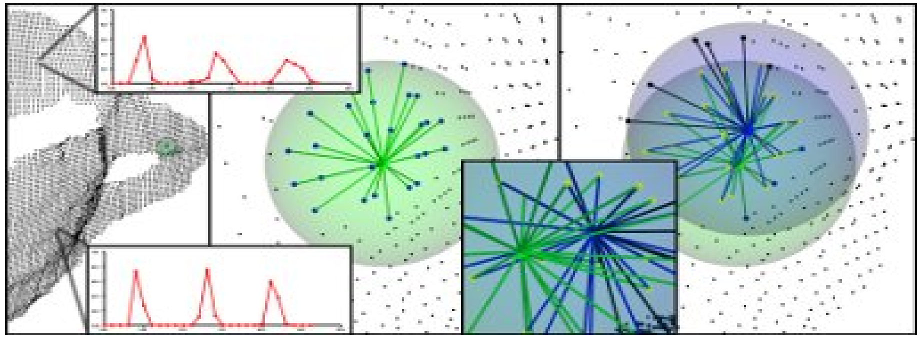

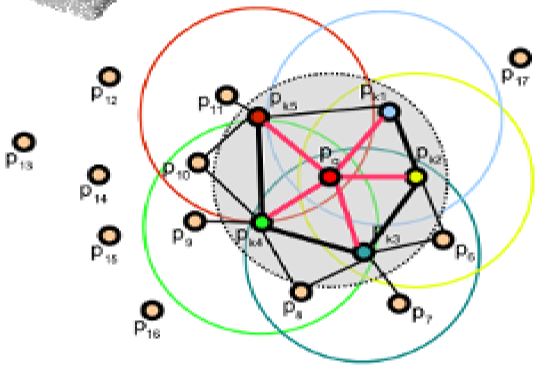

Rusu et al., 2009, 2011

Random Forest - Neural Network

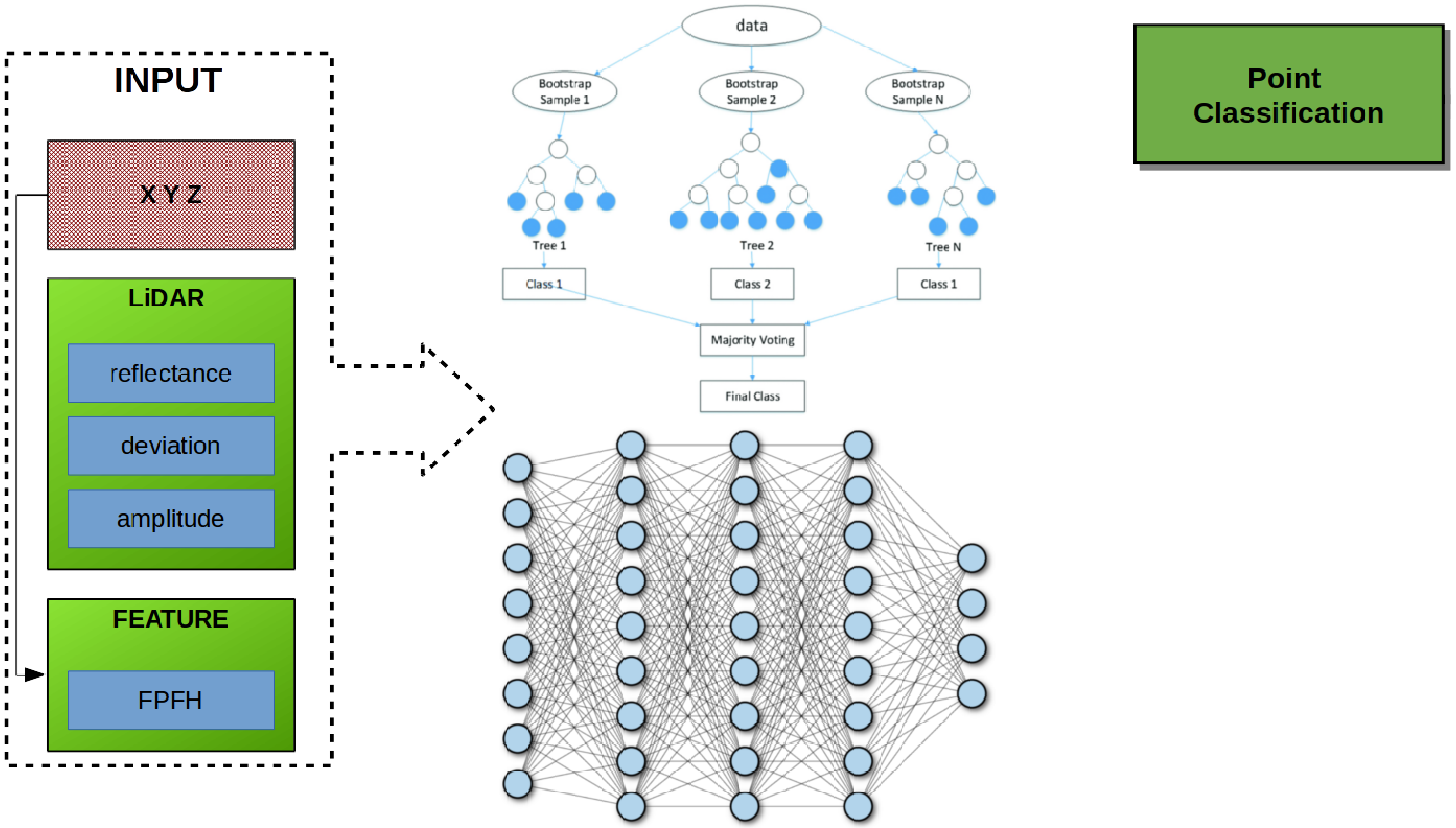

Unsupervised Clustering - DBSCAN

Goals

- Filtering remaining noise
- Identifying each apple instance
  - Count total apples
  - Measure size of apple

Methods

- **DBSCAN**
  - Cluster size
  - Euclidean distance
  - Growing method
- **Hyperparameter optimization**
  - Grid Search

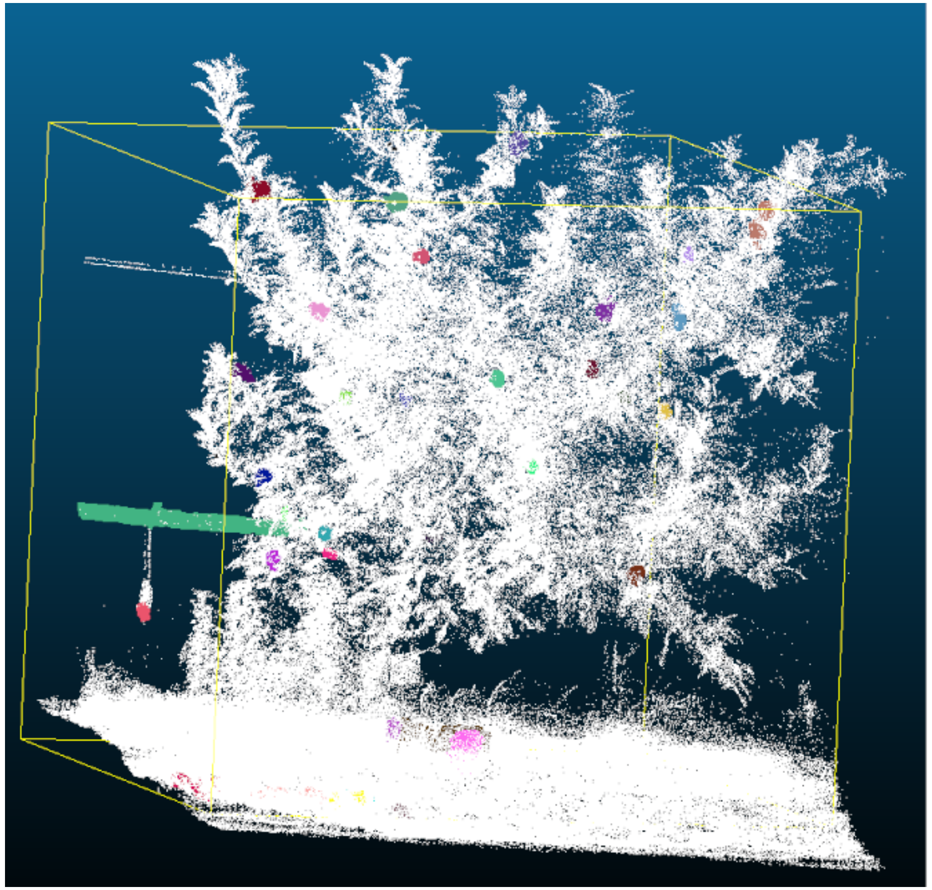

Point Clustering

Deep learning - RandLA-Net

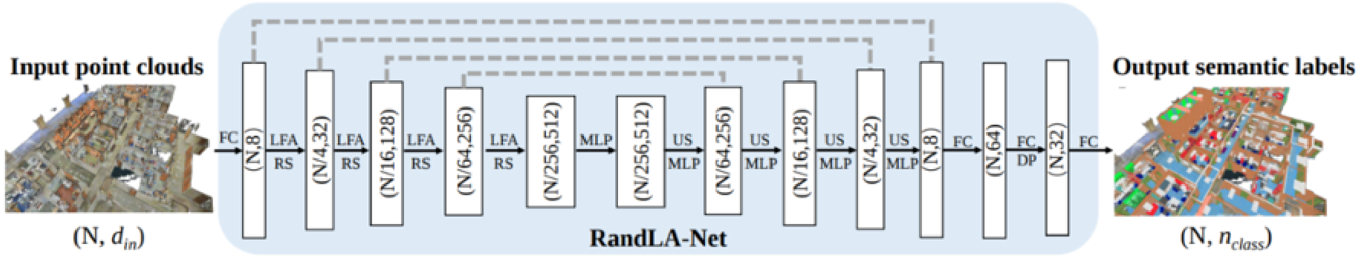

Figure 7. The detailed architecture of our RandLA-Net. (N, D) represents the number of points and feature dimension respectively. FC: Fully Connected layer, LFA: Local Feature Aggregation, RS: Random Sampling, MLP: shared Multi-Layer Perceptron, US: Up-sampling, DP: Dropout.

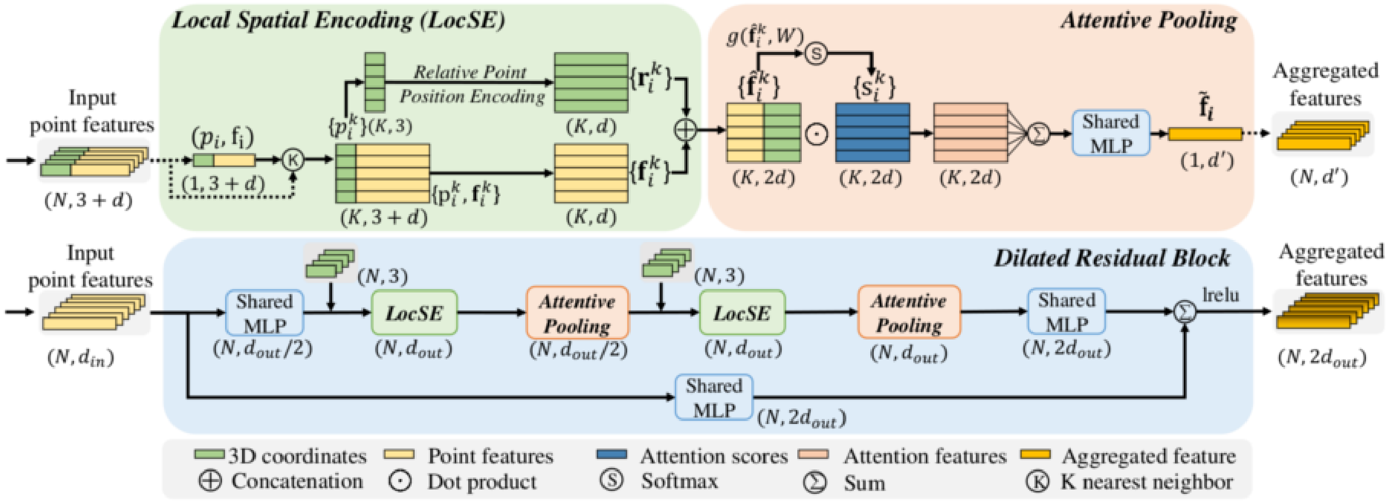

Figure 3. The proposed local feature aggregation module. The top panel shows the location spatial encoding block that extracts features, and the attentive pooling mechanism that weights the most important, based on the local context and geometry. The bottom panel shows how two of these components are chained together, to increase the receptive field size, within a residual block.

Point Characterization

Point Classification

Hu et al., 2020

Results

Results - Model Validation

	Model	Data	feature	MCC	Macro Average F1-Score	Apple F1-Score	Balanced Accuracy	Mean IoU
Machine Learning	Random Forest	field	fpfh + rad	0.27	0.67	0.21	0.82	0.52
		field	fpfh	0.14	0.60	0.11	0.70	0.47
	Neural Network	field	fpfh + rad	0.24	0.66	0.15	0.85	0.48
		field	fpfh	0.14	0.61	0.09	0.74	0.43
Deep learning	RandLA-Net fold_1	field	xyz + rad	0.82	0.91	0.82	0.96	0.85
		field	xyz	0.48	0.74	0.48	0.80	0.64

Point Characterization

Point Classification

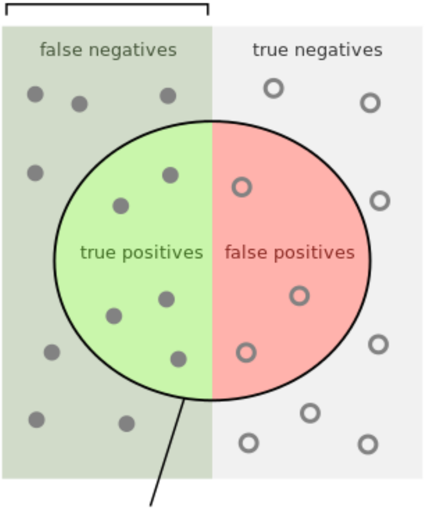

$$MCC = \frac{TP \times TN - FP \times FN}{\sqrt{(TP+FP)(TP+FN)(TN+FP)(TN+FN)}}$$

$$F_1 = \left(\frac{2}{\text{recall}^{-1} + \text{precision}^{-1}}\right) = 2 \cdot \frac{\text{precision} \cdot \text{recall}}{\text{precision} + \text{recall}}$$

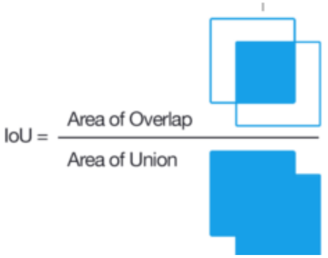

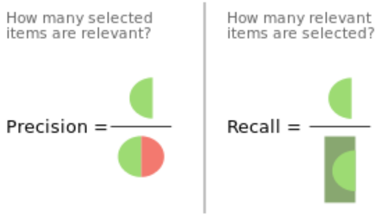

$$\text{Performance} = \frac{1}{5}\sum_{i=1}^{5} \text{Performance}_i$$

Results - Model Validation

	Model	Data	feature	MCC	Macro Average F1-Score	Apple F1-Score	Balanced Accuracy	Mean IoU
Machine Learning	Random Forest	field	fpfh + rad	0.27	0.67	0.21	0.82	0.52
		field	fpfh	0.14	0.60	0.11	0.70	0.47
		Synthetic VeryHiRes	fpfh	0.32	0.66	0.47	0.69	0.50
	Neural Network	field	fpfh + rad	0.24	0.66	0.15	0.85	0.48
		field	fpfh	0.14	0.61	0.09	0.74	0.43
		Synthetic VeryHiRes	fpfh	0.31	0.66	0.45	0.69	0.46
Deep learning	RandLA-Net fold_1	field	xyz + rad	0.82	0.91	0.82	0.96	0.85
		field	xyz	0.48	0.74	0.48	0.80	0.64
		Synthetic VeryHiRes	xyz	0.61	0.80	0.67	0.86	0.62

Point Characterization

Point Classification

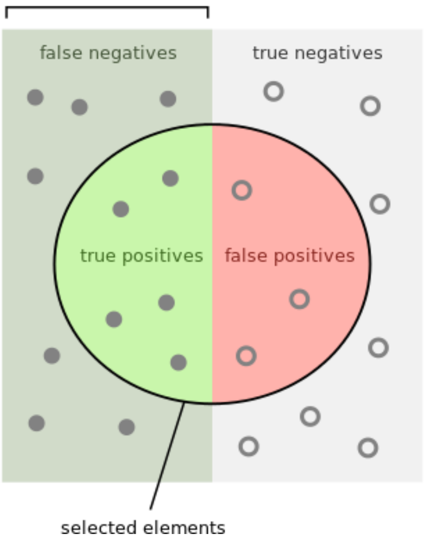

$$MCC = \frac{TP \times TN - FP \times FN}{\sqrt{(TP+FP)(TP+FN)(TN+FP)(TN+FN)}}$$

$$F_1 = \left(\frac{2}{\mathrm{recall}^{-1} + \mathrm{precision}^{-1}}\right) = 2 \cdot \frac{\mathrm{precision} \cdot \mathrm{recall}}{\mathrm{precision} + \mathrm{recall}}$$

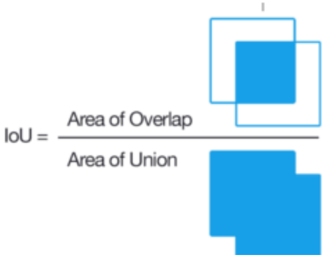

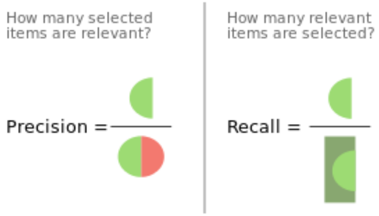

Results - DBSCAN from perfectly labeled synthetic

<u>Pipeline : Ground truth classification + DBSCAN</u>

Synthetic - VeryHiRes

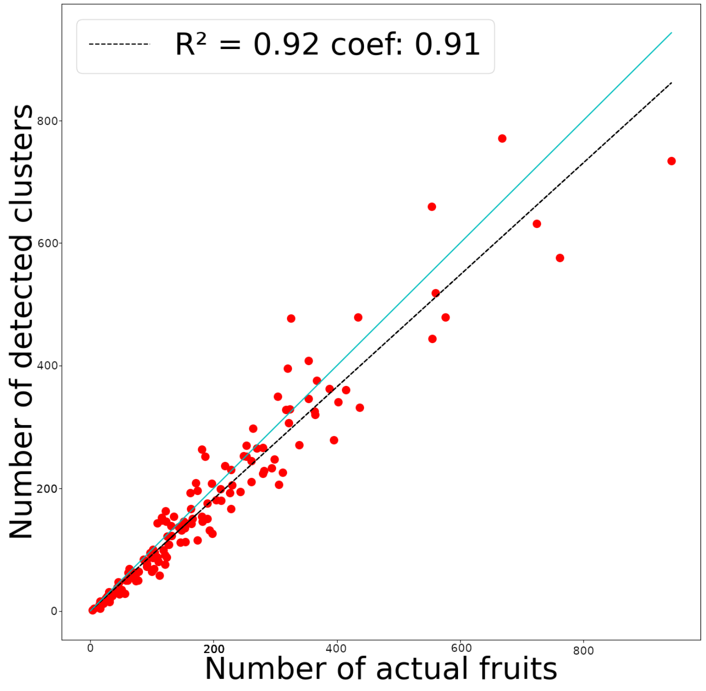

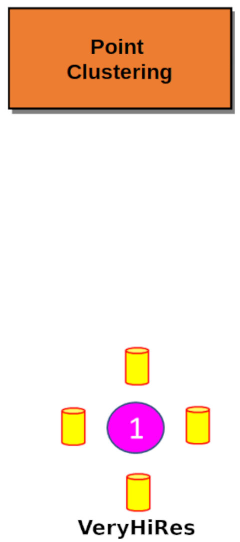

Results - Deep learning pipeline

Pipeline : RandLA-Net + DBSCAN

Synthetic - VeryHiRes

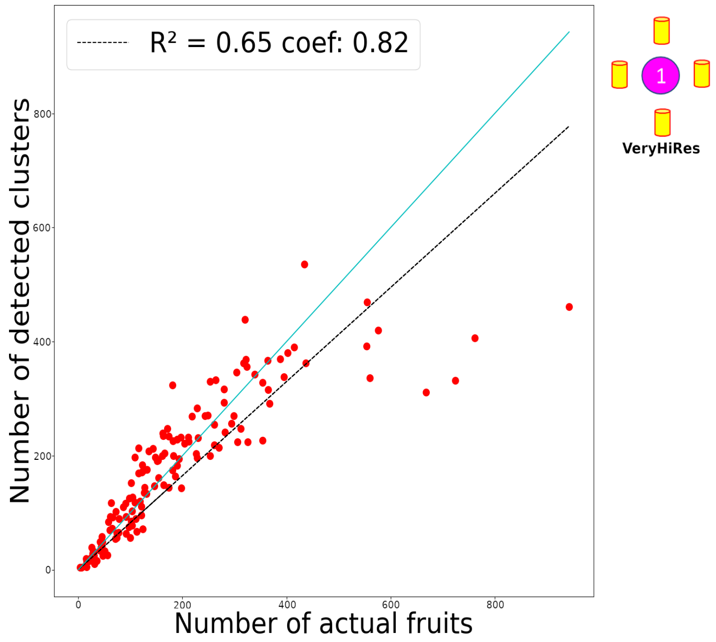

Field - HiRes

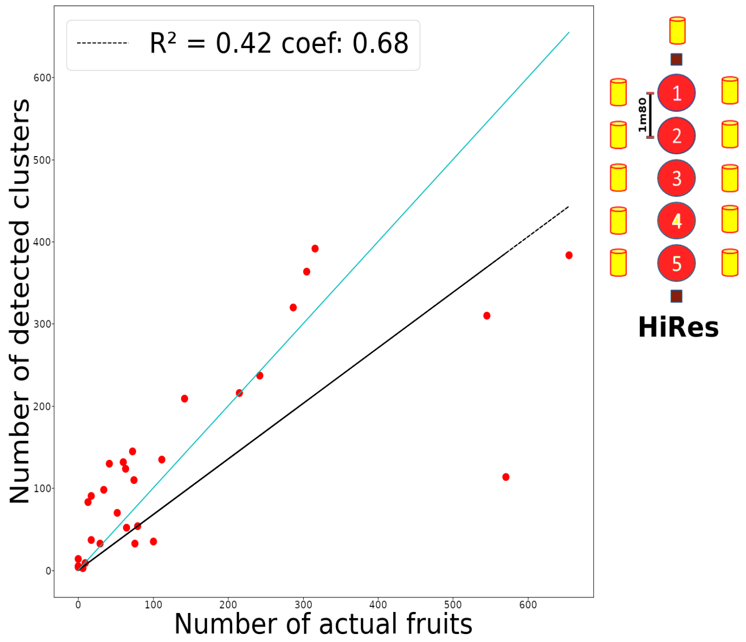

Field - LowRes

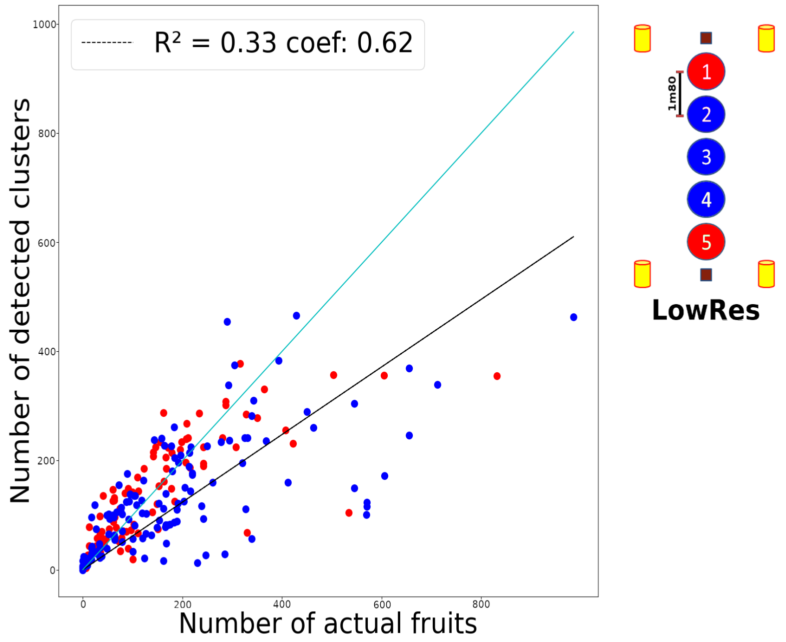

Results - Deep learning pipeline

Pipeline : RandLA-Net + DBSCAN

Field - LowRes
POS 1&5

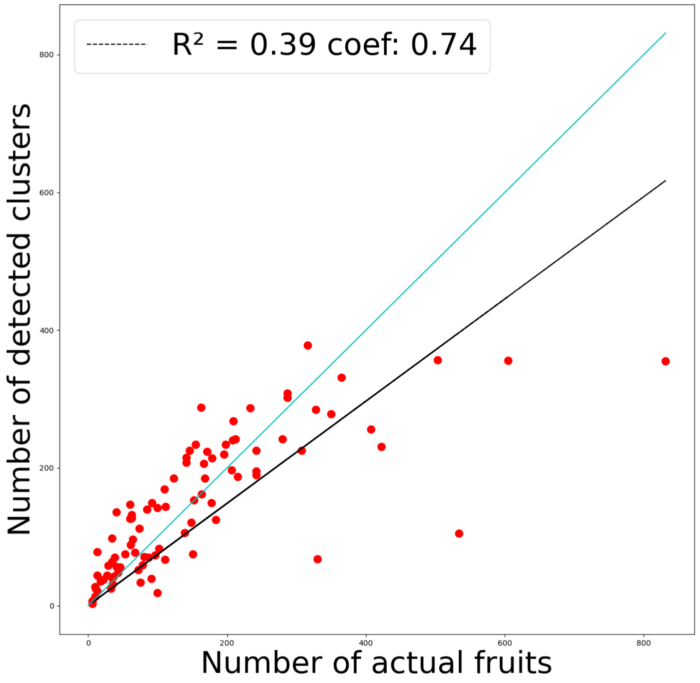

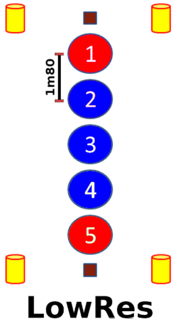

Field - LowRes
POS 2,3,4

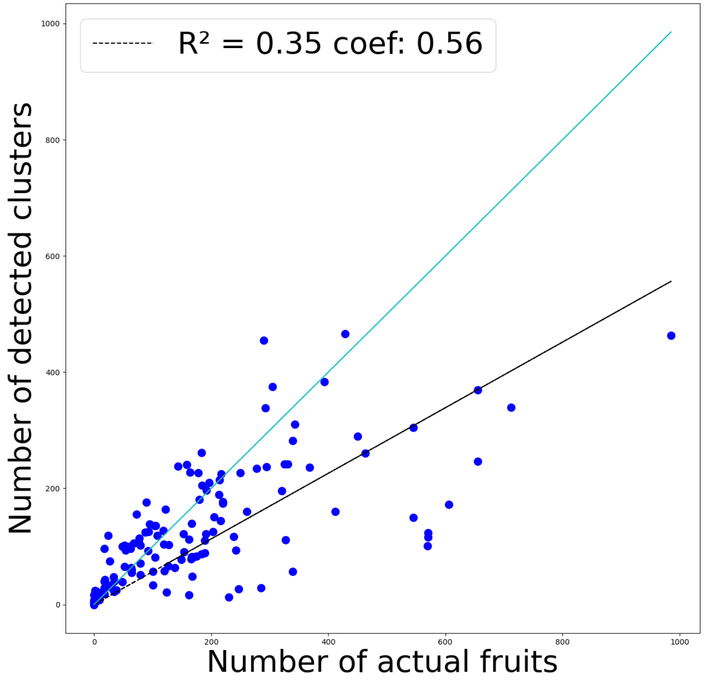

Conclusion

- Importance of the acquisition protocol and LiDAR resolution
- Even with few data, results are promising :
  - Deep learning outperfom machine learning
  - With more training data we can expect better results
- Deep instance segmentation
- Try our method on commercial apple tree orchard
  - Compare with other methods

Thank you

For any questions or more detail please contact us at :

- simon.artzet@gmail.com
- frederic.boudon@cirad.fr

References

- Costes et al., 2008, Functional Plant Biology 35, 936-950, https://doi.org/10.1071/FP08081
- Coupel-Ledru et al., 2019, Horticultural Research, 6-52, https://doi.org/10.1038/s41438-019-0137-3
- Boudon et al., 2014, Annals of Botany 114, 4, 853-862, https://doi.org/10.1093/aob/mcu062
- Pradal et al., 2009, Graphical Models 71, 1-21, https://doi.org/10.1016/j.gmod.2008.10.001
- Ziamtsov et Navlakha, 2019, Plant Physiology 181, 1425-1440, https://doi.org/10.1104/pp.19.00524
- Gene-Mola et al., 2019, Biosystems Engineering 187, 171-184, https://doi.org/10.1016/j.biosystemseng.2019.08.017
- Tsoulias et al., 2020, Remote Sens 12, 2481, https://doi.org/10.3390/rs12152481
- Qi et al., 2017, IEEE CVPR, 77-85, https://doi.org/10.1109/CVPR.2017.16
- Rusu et al., 2009, IEEE, 3212-3217, https://doi.org/10.1109/ROBOT.2009.5152473
- Rusu et al., 2011, IEEE, 1-4, https://doi.org/10.1109/ICRA.2011.5980567
- Pedregosa et al., 2011, Journal of Machine Learning Research 12, 85, 2825-2830, http://jmlr.org/papers/v12/pedregosa11a.html
- Guo, Wang, Hu, Liu et al., 2020, IEEE, 1-1, https://doi.org/10.1109/TPAMI.2020.3005434
- Hu et al., 2020, IEEE, 11105-11114, https://doi.org/10.1109/CVPR42600.2020.01112.
- Breiman, 2001, Machine Learning 45, 5-32, https://doi.org/10.1023/A:1010933404324